

Axial charges of excited nucleons from CI-fermions

T. Maurer¹, T. Burch¹, L. Ya. Glozman², C. B. Lang², D. Mohler³ and A. Schäfer^{1 a}

¹ Institut für Theoretische Physik, Universität Regensburg, D-93040 Regensburg, Germany

² Institut für Physik, FB Theoretische Physik, Universität Graz, A-8010 Graz, Austria

³ TRIUMF, 4004 Wesbrook Mall Vancouver, BC V6T 2A3, Canada

the date of receipt and acceptance should be inserted later

Abstract. We report lattice QCD results on the axial charges of ground and excited nucleon states of both parities. This is the first study of these quantities with approximately chiral (CI) fermions. Two energy levels in the range of the negative parity resonances $N^*(1535)$ and $N^*(1650)$ are observed and we determine the axial charge for both. We obtain a small axial charge for one of them, which is consistent with the chiral symmetry restoration in this state as well as with the small axial charge of the $N^*(1535)$ predicted within the quark model. This result agrees with the findings of Takahashi et al. [1] obtained with Wilson quarks which violate chiral symmetry for finite lattice spacing. At the same time for the other observed negative parity state we obtain a large axial charge, that is close to the axial charge of the nucleon. This is in disagreement both with the quark model prediction as well as with the chiral restoration but allows for an interpretation as an s -wave πN state.

PACS. 12.38.Gc Lattice QCD calculations – 11.30.Rd Chiral symmetries – 14.20.-c Baryons – 21.10.Ky Electromagnetic moments

1 Introduction

With the advent of high luminosity accelerators hadron spectroscopy became again part of the forefront of physics. New states have been observed, e.g., the X,Y,Z bosons by Babar, Belle and Cleo [2,3] which suggest that states exist which have a more complicated lowest-Fock-state parton structure than $\bar{q}q$ (and correspondingly qqq). One extensively discussed possibility is the existence of tetraquarks. One of the issues is where to draw the line between tetraquarks and meson molecules [4,5], or pentaquarks and baryon-meson molecules for that matter. In this context the two negative parity nucleon excitations $N^*(1535)$ and $N^*(1650)$ are of special interest as it is often assumed that they are mixtures of a genuine three quark state and a pentaquark state, which can also be thought of as a molecule [6,7,8,9,10]. So, a better understanding their properties is a topical task. Another one is to improve on hadron spectroscopy in general, and thus to be better able to decide which hadrons do not fit into standard $\bar{q}q$ and qqq phenomenology. One of the major order schemes for the latter is chiral symmetry.

If chirality were a good symmetry of hadron physics, all hadrons would occur in parity pairs, which is obviously not the case. However, one can hope that remnants of chiral symmetry remain. Therefore, it is a much discussed question whether hadron resonances show some statistically relevant degree of parity pairing. The answer seems to be

affirmative, see, e.g., [11], but not indisputable. Therefore, the identifications and measurement of quantities which are sensitive to this issue are important.

In refs. [12,13] it was proposed that the observed parity doubling for higher excitations can be explained via an effective restoration of chiral symmetry and the formation of approximate parity-chiral multiplets. Furthermore, the axial charge of each parity doublet state has to be zero for an exact symmetry. The hypothesis of an effective chiral symmetry restoration can therefore be tested by calculating the axial charges of members of parity doublet resonances [14].

There exists, in fact, circumstantial evidence for the hypothesis of effective chiral restoration. The pion decay rate of nucleon resonances with approximately restored chiral symmetry should be suppressed and, in fact, the decay of probable members of parity doublets was found to be suppressed by a factor of ten [14].

For this and many similar problems in hadron physics it is hoped that lattice QCD will provide crucial clarifications. In particular, the variational analysis method [15,16] has helped considerably to study excited states on the lattice [17,18,19,20,21,22,23,24]. However, finding the correct interpretation of the results of such simulations is always a challenge.

Ideally, given large enough propagation distance in Euclidean time, high enough statistics and a complete set of interpolators, the observed energy levels in the propagator analysis should be well defined. In reality there

^a andreas.schaefer@physik.uni-r.de

always remains a certain dependence on the chosen set of interpolators. Typically, only those states which have a large overlap with one or more of the set become statistically significant. Using just three-quark interpolators for the baryons, it is unclear whether one can observe a noticeable overlap with baryon-meson states, even in simulations with dynamical quarks. As an example for such weak coupling one may refer to the ρ -meson, where only explicit inclusion of p-wave $\pi\pi$ -interpolators lead to corresponding energy levels in the analysis [25]. The stability of the eigenvectors over several time slices helps to identify the eigenstate; however, in the absence of explicit baryon-meson interpolators, one cannot hope to discern the physical content of the state.

Indeed, the expected lowest energy for the s -wave πN channel overlaps with the region of the two lowest negative parity $1/2^-$ states, observed on the lattice by practically all groups. Consequently, one does not know a priori whether the observed two lowest states in dynamical lattice calculations represent the resonances $N^*(1535)$ and $N^*(1650)$ or, in fact, one of the resonances and the $\pi - N$ system in the s -wave. One needs additional dynamical information about these states to resolve the issue. Axial charges of the observed states could help to answer this question.

A study similar to our's was already done some time ago by Takahashi et al. [26] who indeed found that one of the first negative parity nucleon resonances has a very small axial charge. However, these authors used Wilson fermions which violate chiral symmetry for any finite a , which obviously is a cause of concern for this kind of investigation. To clarify the situation we present here a similar study, performed, however, with approximately chiral fermions, so-called CI (chirally improved) fermions. The motivation for the development of this fermion action [27, 28] is that implementing chirality exactly on the lattice introduces unavoidable non-localities which make simulations very expensive. (Such simulations became possible recently, see [29], although only on small lattices.)

The outline of the paper is as follows: In section 2 we will discuss g_A and its calculation on the lattice. In section 3 the variational method used will be presented and lattice details are given in section 4. We present and interpret the numerical results in section 5 and finally summarize our conclusions.

2 The axial charge g_A

In this section we summarize well known facts about the axial charge which provides a background for what will be discussed further on.

The axial charge g_A of the ground state nucleon, or more precisely the ratio g_A/g_V is a central property of this baryon. It describes its coupling strength to the weak interaction and has been deduced, e.g., from neutron β decay [30]:

$$g_A/g_V = 1.2670 \pm 0.0030$$

The neutron β decay involves four form factors (see [31]): vector g_V , tensor g_T , axial g_A and pseudo-scalar g_P :

$$\langle p|V_\mu^+|n\rangle = \bar{u}_p [\gamma_\mu g_V(q^2) - q_\lambda \sigma_{\lambda\mu} g_T(q^2)] u_n \quad (1)$$

$$\langle p|A_\mu^+|n\rangle = \bar{u}_p [\gamma_\mu \gamma_5 g_A(q^2) - i q_\mu \gamma_5 g_P(q^2)] u_n \quad (2)$$

where $V_\mu^+ = \bar{u}\gamma_\mu d$, $A_\mu^+ = \bar{u}\gamma_\mu \gamma_5 d$ and q_μ is the momentum transfer between proton and neutron. In the limit of zero momentum transfer $q^2 \rightarrow 0$ the axial and vector form factors dominate. Their values in this limit are called the vector and axial charges of the nucleon: $g_V = g_V(0)$ and $g_A = g_A(0)$.

We neglect the mass differences of up and down quarks ($m_u = m_d \neq 0$) and hence the neutron and proton mass difference. In this case the global chiral $SU(2) \times SU(2)$ symmetry (when $m = m_u = m_d = 0$) is broken except for the vector $SU(2)$ subgroup. The associated vector charge $g_V = 1$ is still conserved. The axial symmetry is explicitly broken by $m \neq 0$. The lattice calculation of axial charges relies on the conservation of vector symmetry. One can write:

$$\langle p|V_\mu^+|n\rangle = 2\langle p|V_\mu^3|p\rangle = \langle p|V_\mu^u|p\rangle - \langle p|V_\mu^d|p\rangle \quad (3)$$

$$\langle p|A_\mu^+|n\rangle = 2\langle p|A_\mu^3|p\rangle = \langle p|A_\mu^u|p\rangle - \langle p|A_\mu^d|p\rangle, \quad (4)$$

where $V_\mu^{(q)} = \bar{q}\gamma_\mu q$, $A_\mu^{(q)} = \bar{q}\gamma_\mu \gamma_5 q$. This links the weak interaction properties to properties determined by the quark content of the state. The electric charge of the neutron is zero, which implies:

$$0 = \langle n|j^{\text{em}}|n\rangle = \frac{2}{3}\langle n|V^u|n\rangle - \frac{1}{3}\langle n|V^d|n\rangle \quad (5)$$

$$\Rightarrow 2\langle n|V^u|n\rangle = \langle n|V^d|n\rangle \quad (6)$$

Isospin symmetry implies the equivalent equation:

$$2\langle p|V^d|p\rangle = \langle p|V^u|p\rangle. \quad (7)$$

Since the electric charge of the proton is one, we can conclude

$$\langle p|j^{\text{em}}|p\rangle = \frac{2}{3}\langle p|V^u|p\rangle - \frac{1}{3}\langle p|V^d|p\rangle \quad (8)$$

$$= \langle p|V^u|p\rangle - \langle p|V^d|p\rangle = \langle p|V^+|n\rangle. \quad (9)$$

This implies $g_V = 1$ for the nucleon.

We now look at continuum matrix elements of states k of momentum p and spin s , where we normalize $s^2 = -1$ and $p^2 = -m_k^2$. Generally, one defines Lorentz decompositions

$$\langle k|V_\mu^{(q)}|k\rangle = \langle k|\bar{q}\gamma_\mu q|k\rangle = 2v_1^{(k,q)} p_\mu \quad (10)$$

$$\langle k|A_\mu^{(q)}|k\rangle = \langle k|\bar{q}\gamma_\mu \gamma_5 q|k\rangle = a_0^{(k,q)} s_\mu m_k \quad (11)$$

The operator product expansion relates such matrix elements to moments of structure functions:

$$v_n^{(q)} = \int_0^1 dx x^{n-1} [q(x) + (-1)^n \bar{q}(x)] = \langle x^{n-1} \rangle_q \quad (12)$$

$$a_n^{(q)} = \int_0^1 dx x^n [\Delta q(x) + (-1)^n \Delta \bar{q}(x)] = \langle x^n \rangle_{\Delta q}. \quad (13)$$

Here, $v_1^{(k,q)}$ is the 0th moment of the unpolarized quark distribution function $q(x)$ in a state k . It counts the number of quarks q . For nucleons we have

$$g_V = v_1^{(u)} - v_1^{(d)} = 1 = \langle 1 \rangle_{u-d}. \quad (14)$$

Next, $a_0^{(k,q)}$ is the 0th moment of the polarized quark distribution function $\Delta q(x)$ and determines the average spin fraction carried by all quarks q .

$$2g_A = a_0^{(u)} - a_0^{(d)} = \langle 1 \rangle_{\Delta u - \Delta d}. \quad (15)$$

If we work with states of zero momentum, we get direct access to these interesting quantities:

$$\langle \mathbf{p} | V_0^{(u-d)} | \mathbf{p} \rangle = 2g_V p_0 \quad (16)$$

$$\langle \mathbf{p}, \mathbf{s} | A_i^{(u-d)} | \mathbf{p}, \mathbf{s} \rangle = 2g_A m_p s_i \quad (17)$$

In lattice normalization $\langle \mathbf{p}, \mathbf{s} | \mathbf{p}, \mathbf{s} \rangle = 1$ one has

$$\langle \mathbf{p} | V_0^{(u-d)} | \mathbf{p} \rangle = g_V \quad (18)$$

$$\langle \mathbf{p}, \mathbf{s} | A_i^{(u-d)} | \mathbf{p}, \mathbf{s} \rangle = g_A s_i \quad (19)$$

where $s^2 = -1$.

3 Variational Method

On the lattice one automatically obtains results for nucleons of opposite parity. The periodicity of the lattice allows propagation backwards in time, which due to $\mathcal{T} \sim \mathcal{PC}$, corresponds to the propagation of antinucleons of opposite parity. So, for $0 < t < L_T$ the two-point correlator is dominated by different parity states for small and large t values. For both regions one gets a superposition of ground and excited states. To extract specific excited states from this superposition is in general difficult because in Euclidean space-time they are exponentially suppressed with respect to the ground state by a factor $\exp(-\Delta E t)$, where ΔE is the energy difference. The standard tool to deal with this problem is the variational method [15], which has proven to be more reliable than multi-exponential fits. In this method one chooses a set of interpolators O_i with the quantum numbers of the state of interest and constructs a correlation matrix

$$C_{ij}(t) = \langle O_i(t) \bar{O}_j(0) \rangle. \quad (20)$$

This matrix has a decomposition

$$C_{ij}(t) = \sum_n \langle 0 | O_i | n \rangle \langle n | \bar{O}_j | 0 \rangle e^{-tE_n}. \quad (21)$$

It can be shown [15], that the eigenvalues of the generalized eigenvalue problem

$$C(t) \psi_k(t) = \lambda_k(t, t_0) C(t_0) \psi_k(t) \quad (22)$$

behave as

$$\lambda_k(t, t_0) = c_k e^{-(t-t_0)E_k} \left(1 + \mathcal{O} \left(e^{-(t-t_0)\Delta E_k} \right) \right), \quad (23)$$

while $\lambda_k(t_0, t_0) = 1$. At fixed t_0 , ΔE_k is given by

$$\Delta E_k = \min\{E_m - E_n | m \neq n\}. \quad (24)$$

For the special case of $t \leq 2t_0$ and a basis of N correlators [32] ΔE_k is given by

$$\Delta E_k = E_{N+1} - E_n. \quad (25)$$

Therefore, at large time separations, each eigenvalue is dominated by a single state, since the difference $E_{N+1} - E_n$ is large. This allows for stable exponential fits to the eigenvalues. Consequently, for large enough Euclidean time t , the largest eigenvalue decays with the mass of the ground state, the second largest eigenvalue with the mass of the first excited state, and so on.

The effectiveness of this method depends crucially on the choice of operators. These must be sufficiently diverse to span a functional space large enough to have good overlap with all states of interest. At the same time the basis cannot be chosen too large as this results in large numerical fluctuations.

We used a basis of six nucleon interpolators, combining two different spinor structures with three different levels of smearing (narrow, medium and wide). The two spinor structures are

$$N_\alpha(t, \mathbf{p}) = \sum_{\mathbf{x}} e^{-i\mathbf{p}\mathbf{x}} \epsilon^{abc} \Gamma_1 u_a(\mathbf{x}, t) (u^b(\mathbf{x}, t)^T \Gamma_2 d^c(\mathbf{x}, t) - d^b(\mathbf{x}, t)^T \Gamma_2 u^c(\mathbf{x}, t)), \quad (26)$$

where table 2 lists the chosen Dirac matrices. Interpolator

type	Γ_1	Γ_2
χ_1	$\mathbf{1}$	$C\gamma_5$
χ_2	γ_5	C

Table 2. The structure of the two variants of nucleon interpolators used. C denotes charge conjugation.

χ_1 contains a scalar diquark (this scalar "diquark" in the local interpolator has nothing to do with the possible clustering in the physical state), while interpolator χ_2 contains a pseudo-scalar diquark. Interpolator χ_1 couples to the nucleon ground state, while the negative parity states are seen with interpolators χ_1 and χ_2 [34, 18].

The three levels of smearing are indicated by a superscript I, \bar{I} . More precisely, the two-point-function of a nucleon with momentum \mathbf{p} , parity \pm , created at time 0 with quark smearings $\bar{I} = (\bar{I}_1, \bar{I}_2, \bar{I}_3)$ and annihilated at time t with quark smearings $I = (I_1, I_2, I_3)$ is denoted by:

$$C_{\alpha\bar{\alpha}}^{I, \bar{I}}(t, \mathbf{p}) = \langle N_\alpha^I(t, \mathbf{p}) \bar{N}_{\bar{\alpha}}^{\bar{I}}(0, \mathbf{p}) \rangle \quad (27)$$

In order to extract the expectation value of some operator \mathcal{O} in a hadron state we determine the 3-point correlation matrix

$$C_{ij}^{\mathcal{O}}(\tau, t) = \langle B_i(t) \mathcal{O}(\tau) \bar{B}_j(0) \rangle \quad (28)$$

lattice	β	$a m_0$	a/fm	a/GeV^{-1}	$a m_{\text{AWI}}$	$m_{\text{AWI}}/\text{MeV}$	N_{cfg}
A50	4.70	-0.050	0.15032(112)	0.7619(57)	0.03027(8)	39.73(10)	200
C64	4.58	-0.064	0.15831(127)	0.8023(64)	0.02995(20)	37.33(25)	200
C72	4.58	-0.072	0.15051(115)	0.7627(58)	0.01728(16)	22.65(21)	200
C77	4.58	-0.077	0.14487(95)	0.7342(48)	0.01054(19)	14.35(26)	300

Table 1. Parameters of our dynamical CI configurations.

and compute ratios (see the simplest variant from [35])

$$R_k(\tau, t) = \frac{\psi_k(t)^\dagger C^\mathcal{O}(\tau, t) \psi_k(t)}{\psi_k(t)^\dagger C(t) \psi_k(t)} \quad (29)$$

$$= \frac{c_k \langle k | \mathcal{O} | k \rangle e^{-tE_k}}{c_k e^{-tE_k}} = \langle k | \mathcal{O} | k \rangle \quad (30)$$

to cancel the exponential factors. These ratios should be τ independent, leading to a plateau-type behavior between time zero and t . The quality of this plateau is the standard test for the precision one has obtained. Altogether we calculate

$$g_{A,V}^{\pm, \text{ren}} = Z_{A,V} g_{A,V}^\pm = \frac{\text{Tr } P_\pm \Gamma^{A,V} \langle N(t) J_\mu^{A,V}(\tau) \bar{N}(0) \rangle}{\text{Tr } P_\pm \langle N(t) \bar{N}(0) \rangle} \quad (31)$$

with $\Gamma_V = \gamma_\mu$ and $\Gamma_A = \gamma_\mu \gamma_5$, and the parity projectors

$$P_\pm = \frac{1 + \gamma_t}{2}. \quad (32)$$

(We choose the time direction $t = 1$.)

For the different sources the corresponding matrix of three-point functions reads

$$C_{\alpha\bar{\alpha}}^{I, \bar{I}, J_\Gamma^{(q)}}(\tau, t, \mathbf{p}) = \langle N_\alpha^I(t, \mathbf{p}) J_\Gamma^I(\tau) \bar{N}_{\bar{\alpha}}^{\bar{I}}(0, \mathbf{p}) \rangle. \quad (33)$$

with the flavor neutral current operators at time τ

$$J_\Gamma^{(q)} = \sum_{\mathbf{x}} \bar{q}_{\delta'}^{\bar{d}}(\mathbf{x}, \tau) \Gamma_{\delta'\delta}^{\bar{d}d} q_\delta^d(\mathbf{x}, \tau). \quad (34)$$

Only connected contributions are relevant to our flavor non-singlet matrix elements.

4 Lattices

We present results for four ensembles of $16^3 \times 32$ lattices and used the tadpole-improved Lüscher-Weisz gauge action, the CI Dirac operator and $n_F = 2$ dynamical quarks, see table 1. (For more details on the setup cf. [17, 36].)

Lattice spacings have been calculated in [33] using the method proposed by Sommer [37, 38] where the Sommer scale was chosen to be $r_0 = 0.48 \text{ fm}$. AWI-masses extrapolated to the physical point have been determined in [33].

We employed one step of stout smearing [39] and three steps of hypercubic-blocking [40] on the gauge configurations, then calculated the two- and three-point functions.

In order to improve the overlap of our operator with real spatially extended states, we choose Jacobi smearing

lattice	identifier	κ	N	r_{RMS}/a
C77	1	0.223	15	2.30(1)
C77	2	0.184	70	4.67(7)
C77	3	0.15	10	0.665(2)
C72	1	0.28	7	1.604(3)
C72	2	0.1925	37	3.493(33)
C72	3	0.4	2	0.8052(6)
C64	1	0.28	7	1.603(4)
C64	2	0.1918	37	3.463(28)
C64	3	0.4	2	0.8052(8)
A50	1	0.223	15	2.30(1)
A50	2	0.184	70	4.66(8)

Table 3. Variety of Gaussian smearings employed. Errors denote standard deviations.

[41, 42]. Table 3 shows the values used, along with the resulting RMS radii. The capital letter always represents the β value, the two numbers symbolize the value of the bare quark mass parameter $a m_0$.

In order to reduce contamination from back-propagating states, we used a Dirichlet boundary condition at t_D , i.e., we modified the gauge configuration by setting all gauge links from t_D to $t_D + 1$ to zero,

$$U_t(t_D, x, y, z) = 0 \quad (35)$$

before inverting any sources. (This was also done in [1].) When we calculated the lattice pion correlator we noticed deviations from a perfect exponential decay behavior at times $|t - t_D| < 6$. For this reason we chose $t_D = 21$ such that there is no influence from the boundary condition in the interval $t \in (0..15)$. We used an implementation of the EigCG inverter [43] to speed up to calculation of propagators for different sources on the same configuration. For each configuration we calculated standard propagators and sequential propagators with all source smearings listed in table 3. We calculated sequential propagators for each $\tau \in \{2, 3, 4\}$ and $\Gamma \in \{\gamma_4, \gamma_3 \gamma_5\}$ to allow a determination of matrix elements of J^V and J^A and hence g_V and g_A . Results for g_V are only available for configuration ensembles C64 and C72.

5 Numerical Results

5.1 Nucleon Masses

We look at positive and negative parity nucleon masses. From an inspection of diagonal elements of the correlation matrix C_{ij} we find: For the positive parity nucleon, only interpolator χ_1 heavily couples to the ground state

for all available smearing types. Interpolator χ_2 couples to excited states predominantly. For the negative parity nucleon, interpolators with χ_1 and χ_2 couple to the ground state for all available smearings. For the negative parity states we observe weaker signals than for the positive parity states. We calculate the full correlation matrix C_{ij} and employ the variational method.

The use of a reference matrix $C_0 \equiv C(t_0)$ in the variational method, discussed in [15, 16], degrades the eigenvalue signals at the benefit of improved signal separation for excited states. We use $t_0 = 1$ for the positive parity states since the signal is stable enough for such a tradeoff. For the negative parity states we use the variational method as well, but employ its trivial variant where $C_0 = 1$.

We diagonalized $C(t)$ for every t and plotted the resulting eigenvectors and eigenvalues, as well as corresponding effective masses. For each of the configurations we have full matrices and results available.

We employed the same smearing parameters as the authors of [36]. Additionally we added a third smearing whose RMS radius is half the size of smallest one. We found no effects on the masses, but the plateaus of three-point over two-point functions become more stable when we include this very narrow smearing.

In the following we discuss only the results for the lowest two states of each parity because we did not obtain stable mass plateaus for the higher excited states. We also show only results for the C77 and C64 ensembles. Those for the other two look very similar.

We plot results for all these subsets in figures 1, 2 and 3, 4. The color-coding in all of these figures is as follows: In the (a) and (b) figures the two lowest energy eigenstates are always drawn in black and red. In the (c) and (d) figures the coefficients for source χ_1 and the three different smearings used are presented in green (narrow), black (medium), red (wide). Those for the source χ_2 are dark purple (narrow), blue (medium), light purple (wide),

Unfortunately our limited computer resources allowed us to generate only 200 configurations for each ensemble, which is clearly not enough for a precise study of excited states. In this case, however, the precise values of g_A for the negative parity states is not so relevant, but rather their approximate size. The question we want to answer is whether there is a negative parity state with an unusually small g_A . Inspecting the plots Figs. 1 to 4 one should not only look at the mass plateaus but also at the eigenvectors obtained by solving the generalized eigenvalue problem. If these vectors are stable one has a reasonable approximation of the eigenstate in question, even if the mass plateaus look marginal. With this in mind we conclude that the only state which is precisely extracted is the positive parity ground state. Its eigenvector composition is dominated by spinor structure χ_1 with a mixture of smearing radii 1 and 2.

For negative parity we clearly obtain two distinct states, characterized by quite different eigenvectors, the masses of which are, however, almost degenerate with rather shaky mass plateaus. This is similar to our previous results, as

ensemble	parity	state	fit interval	am
C77	+	1	2-11	0.691(47)
C77	+	2	2-6	1.564(48)
C77	-	1	1-5	1.07(19)
C77	-	2	1-5	1.08(14)
C72	+	1	2-11	0.881(21)
C72	+	2	2-6	1.772(20)
C72	-	1	1-5	1.451(79)
C72	-	2	1-6	1.350(63)
C64	+	1	2-11	1.033(6)
C64	+	2	2-6	1.806(18)
C64	-	1	1-5	1.65(2)
C64	-	2	1-5	1.59(2)
A50	+	1	2-11	0.974(18)
A50	+	2	2-6	1.585(35)
A50	-	1	1-7	1.19(16)
A50	-	2	1-7	1.340(85)

Table 4. Nucleon masses measured. Fit intervals include data points at their boundaries.

well as to results of other groups. Typically these two observed states are interpreted as the resonances $N^*(1535)$ and $N^*(1650)$. However, at our quark masses the S-wave πN state lies in the same region. Consequently, we do not know whether these two observed lattice states represent the resonances $N^*(1535)$ and $N^*(1650)$, or one of these resonances and the S-wave πN state.

The first-excited positive parity state (the Roper) is not well reproduced. Its mass is much too high and its eigenvector composition is rather unstable. This is a problem shared by many other lattice studies [23]. Very recent results suggest that these problems are caused by finite volume artefacts, which, if so, should be especially large for our comparably small lattices. This could indicate some special properties of the Roper wave function which are not yet fully understood (e.g., a strong coupling to more-extended Fock states).

In order to extract the masses of the states we performed a double exponential fit to

$$\lambda(t) = A_1 e^{-m_1 t} + A_2 e^{-m_2 t} \quad (36)$$

for each set of eigenvalues, such as to correct for the higher state admixtures clearly visible at small t . Table 4 contains always the lower mass value for each such fit.

To compare to physical masses one still has to perform a chiral extrapolation. As our statistics are insufficient to do this with reasonable precision, we simply plot the masses we obtained as a function of the axial Ward identity (AWI) quark mass in figure 5.

5.2 Baryon Charges

In Figs. 6 – 11 we show our results for the vector and axial charge for nucleons of both positive and negative parity. The three curves in the plots differ by the value of τ chosen in 31. All curves should reach the same plateau for times $t \geq \tau$, which they do. The values $\tau = 3, 4$ and 5 correspond to the black, red and green lines, respectively.

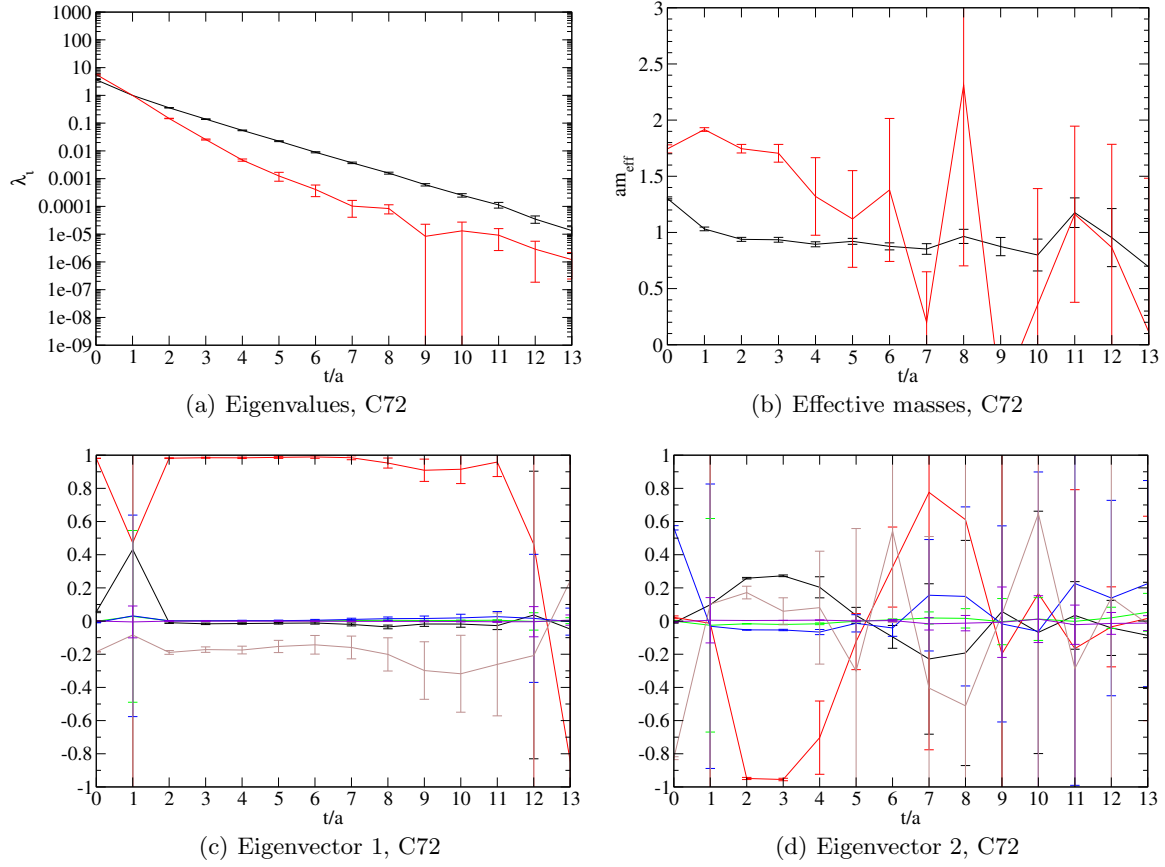


Fig. 1. Results for the two lowest positive parity states for ensemble C72.

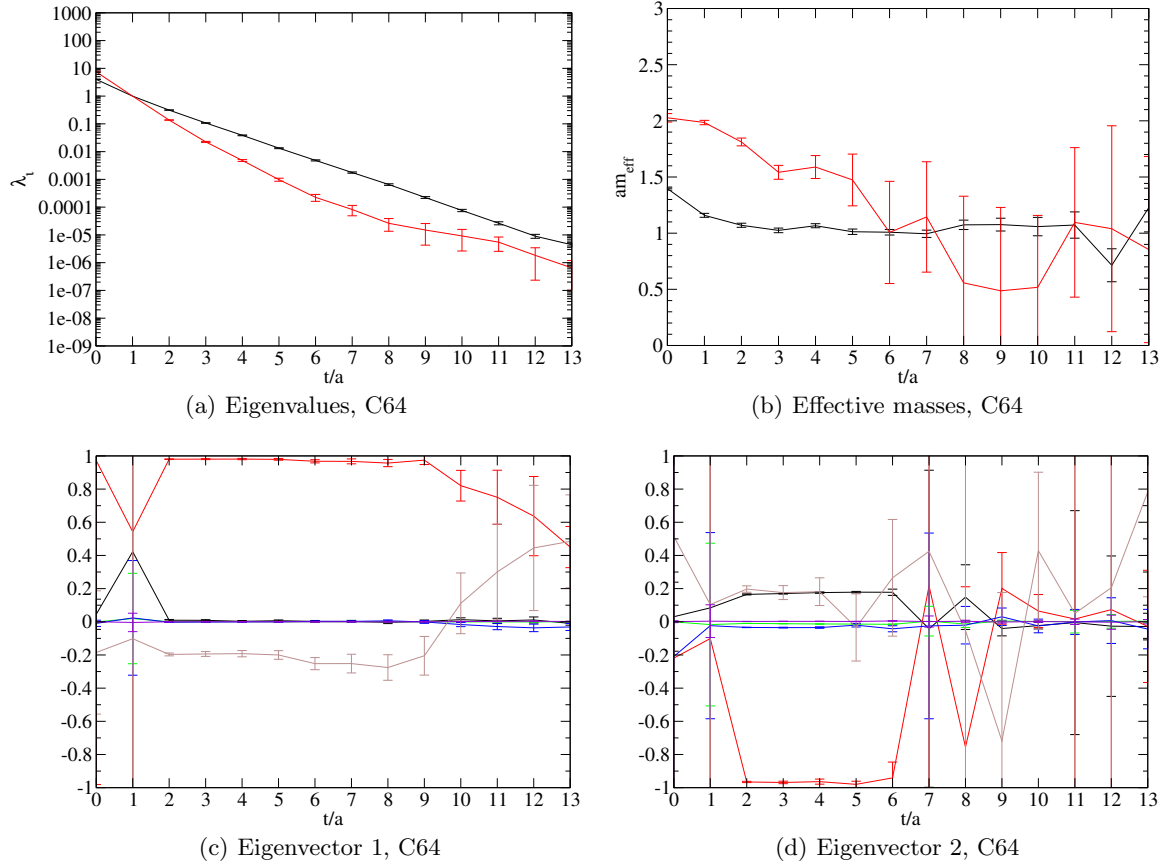
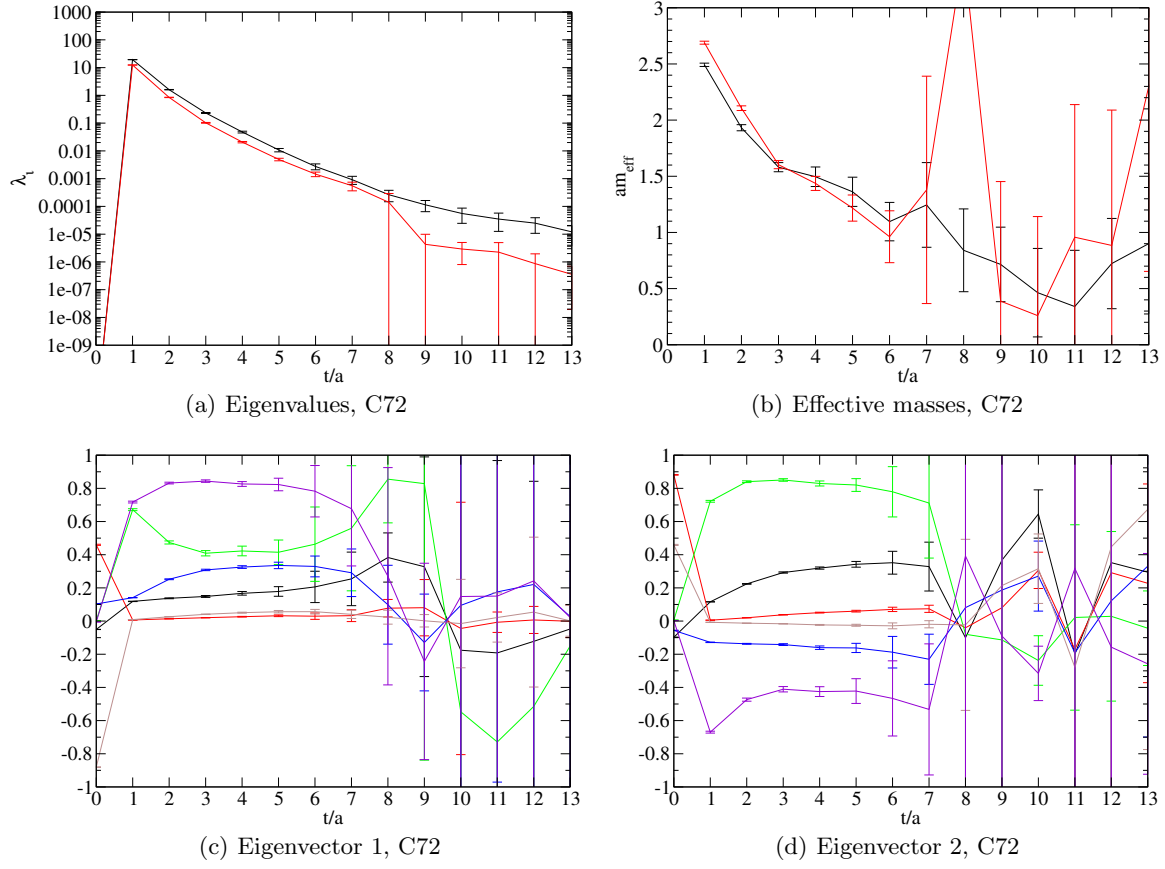
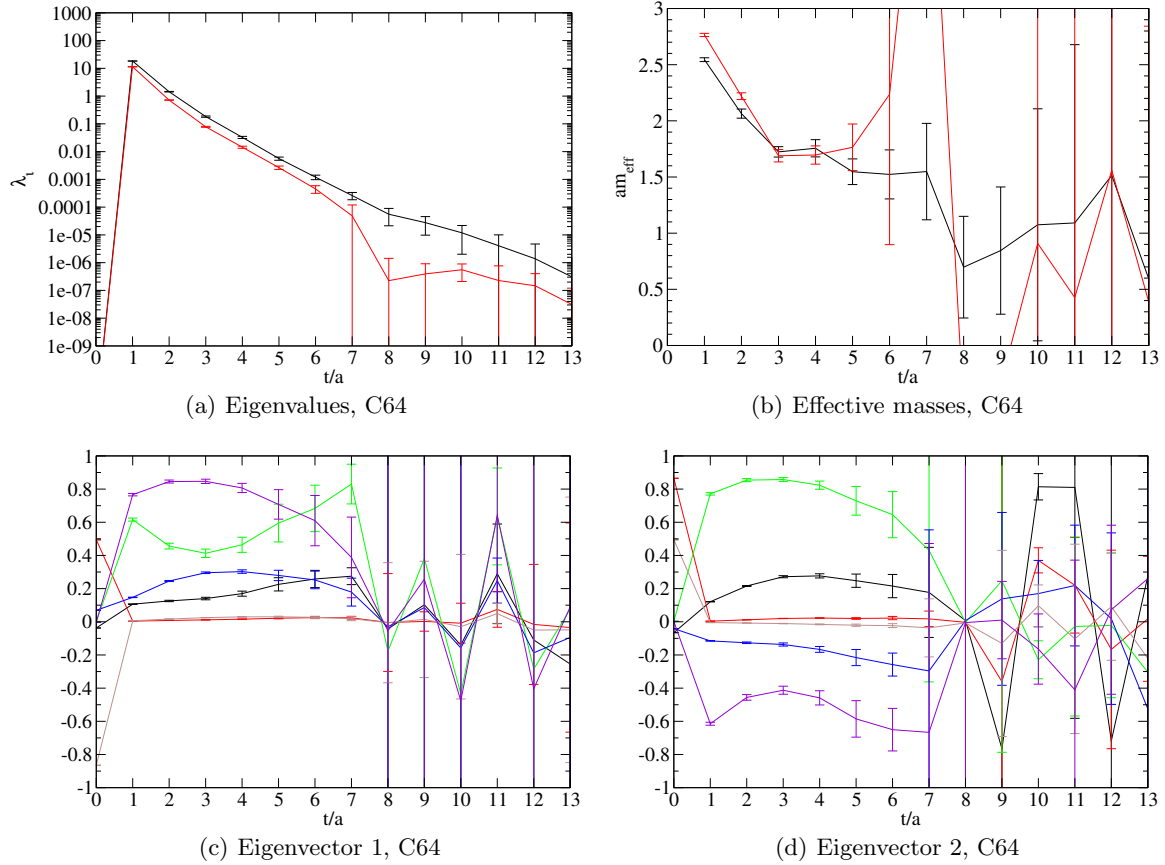


Fig. 2. Results for the two lowest positive parity states and ensemble C64.

**Fig. 3.** Results for the two lowest negative parity states for ensemble C72.**Fig. 4.** Results for the two lowest negative parity states and ensemble C64.

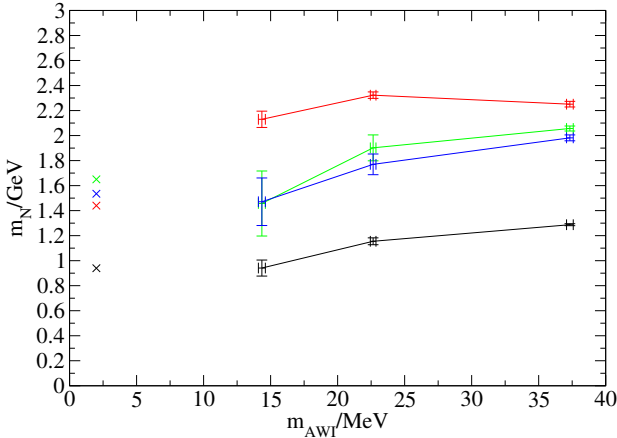


Fig. 5. Dependence of the nucleon masses on the AWI quark mass (ensembles C77, C72 and C64). Shown are the lowest two states of positive and negative parity.

In each plot we show ratios of three-point over two-point functions for the state composition determined by the eigenvector obtained from the variational method. The operators chosen are γ_4 for the vector charge and $\gamma_3\gamma_5$ for the axial vector one. We will comment on the renormalization factors below.

In all cases presented the behavior is the same for times above the chosen t : the vector and axial vector charges form plateaus at values which are compatible for all ensembles and all choices of t and thus should be physical. However, even when one gets a reasonable plateau, data are quite noisy and the list of results given in table 5 should be interpreted with care. Still, it seems clear that one of the negative parity states has indeed a very small axial charge. This confirms the lattice results of [1].

We determined the renormalization factors

$$g_A^{\text{ren}} = Z_A g_A, \quad (37)$$

$$g_V^{\text{ren}} = Z_V g_V. \quad (38)$$

in a separate analysis [44].

As a check of the accuracy of our calculations we give in Table 5 also the renormalized vector charges for two of our ensembles. The deviation from 1, which is of the order 0.05 should be taken as estimate for the systematic uncertainties of our calculation, which is substantially larger than the purely statistical error given in brackets. We thus assume that also our results for g_A have an systematic uncertainty of about 0.05 in addition to the statistical uncertainties quoted.

As stated above our data are insufficient for simultaneous continuum and chiral extrapolations. Since we have data for three quark masses for ensemble C, we can attempt a linear extrapolation, see Fig. 12 and table 6. This gives at least a rough feeling for the size of the effects of a chiral extrapolation. Table 6 gives the main results of our investigation. The value for g_A for the ground state $N(939)$ comes out a bit too low, which again is a common problem for many lattice calculations of this quantity. It is known that g_A is very sensitive to finite size corrections [45, 31, 46, 47, 48, 45, 49, 50], which reduce its value.

lat.	prty.	state	time	$g_A = Z_A R_A$	$g_V = Z_V R_V$
C77	+	0	4	1.137(13)	-
C77	+	1	4	0.788(165)	-
C77	-	0	5	1.032(99)	-
C77	-	1	5	0.121(128)	-
C72	+	0	4	1.164(10)	1.036(3)
C72	+	1	4	0.733(194)	0.946(104)
C72	-	0	5	0.897(65)	1.066(10)
C72	-	1	5	-0.053(78)	1.074(11)
C64	+	0	4	1.175(11)	1.027(2)
C64	+	1	4	0.960(26)	1.019(8)
C64	-	0	5	0.858(73)	1.058(7)
C64	-	1	5	-0.022(82)	1.061(11)
A50	+	0	4	1.178(9)	-
A50	+	1	4	1.024(32)	-
A50	-	0	5	0.891(48)	-
A50	-	1	5	-0.145(71)	-

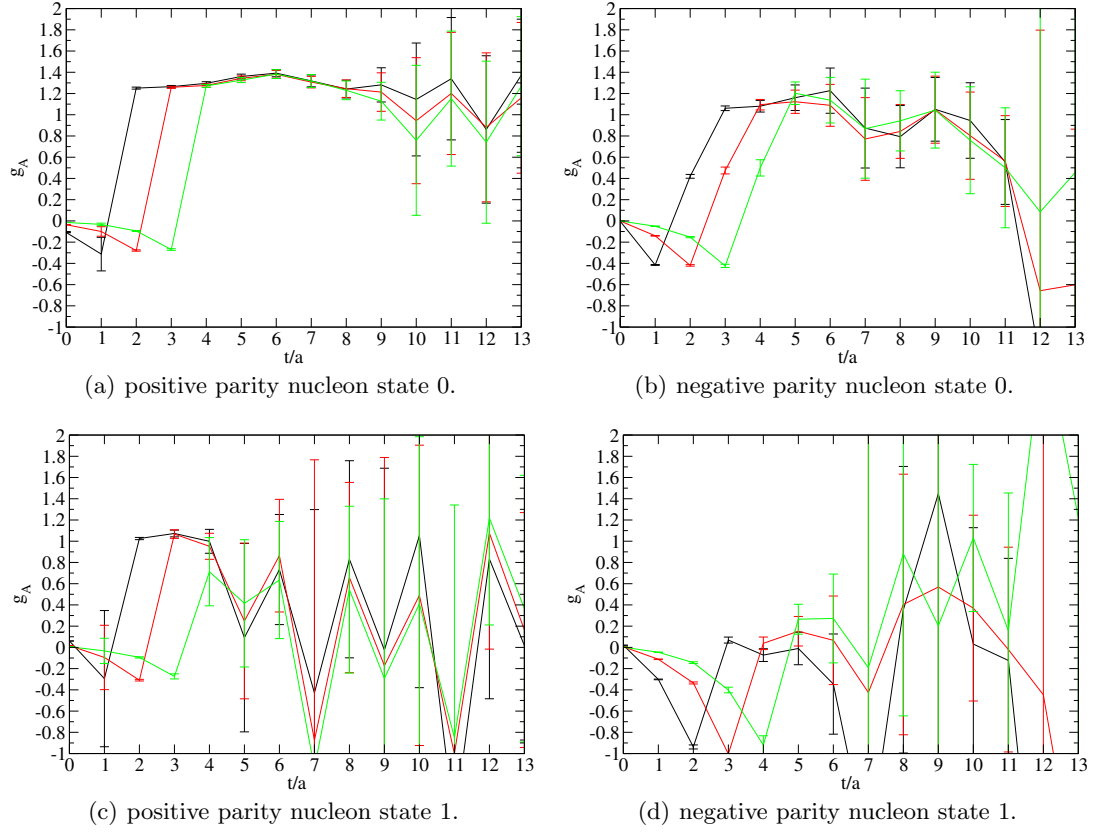
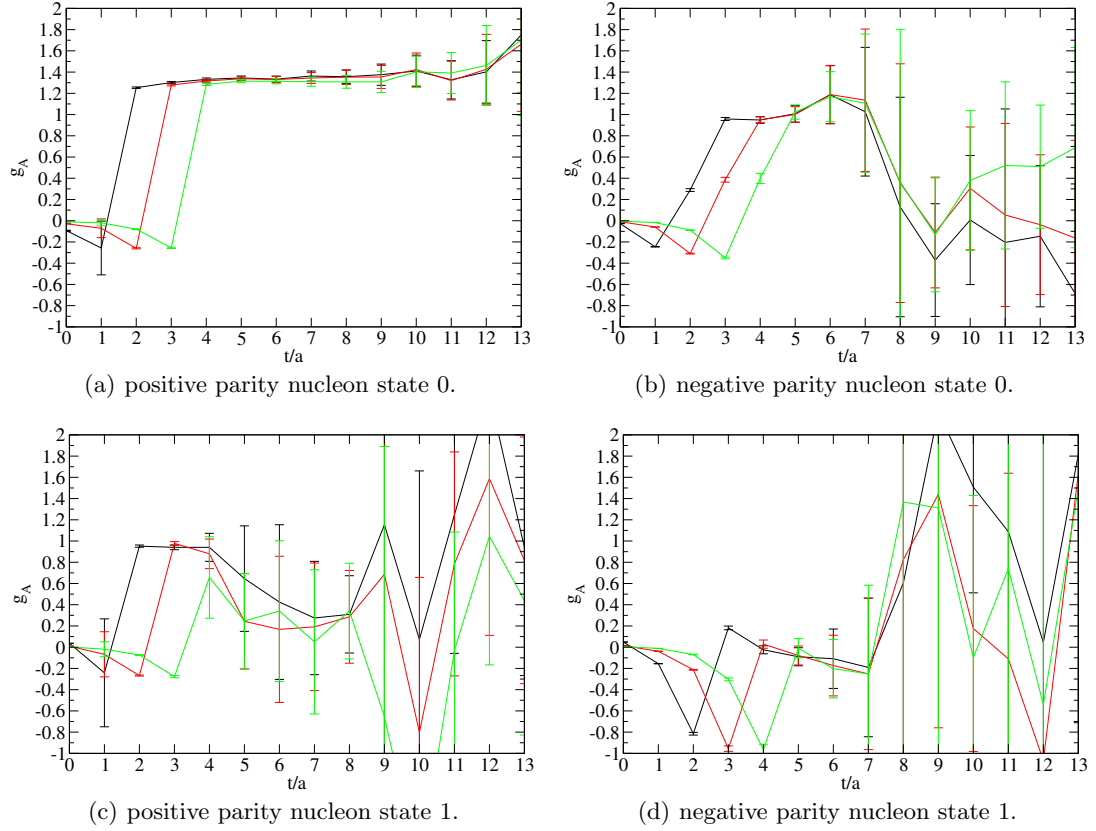
Table 5. Renormalized axial and vector charges. Renormalization factors were taken from [44].

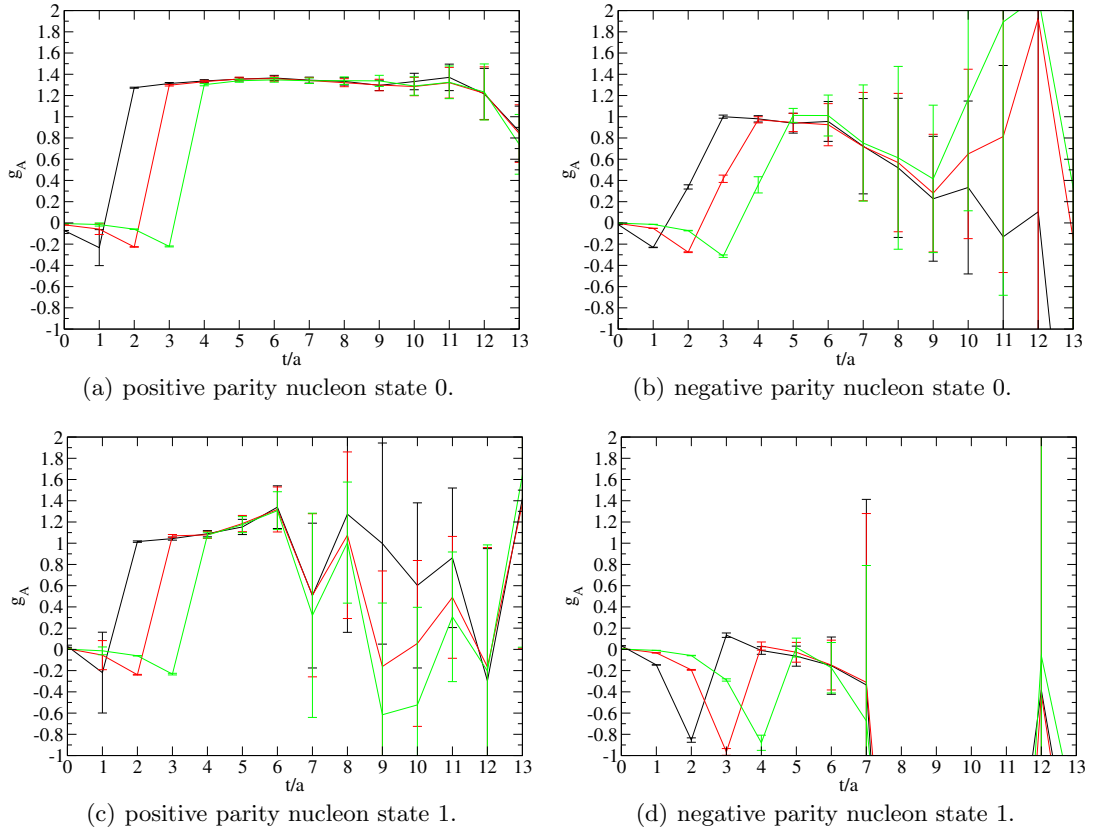
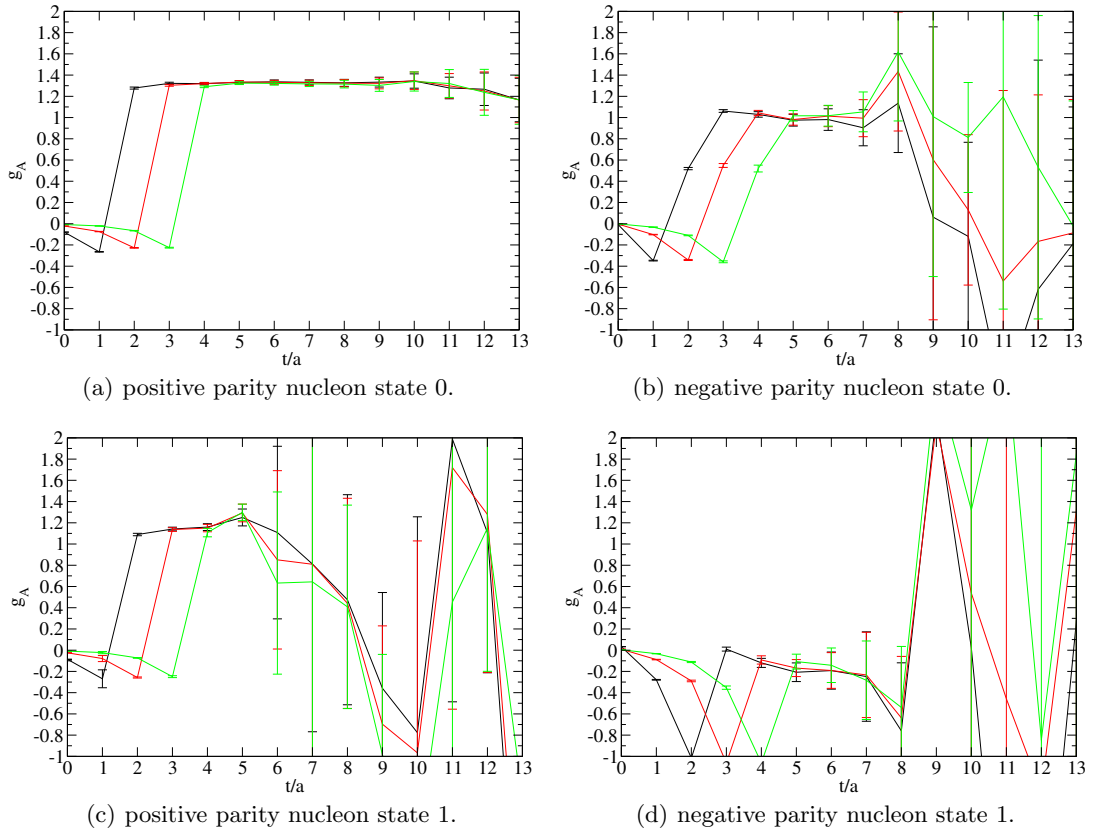
This fact is again related to larger higher-Fock-state admixtures, which in this case may also be described in terms of the pion cloud [51]. As our lattices are rather small ($L \sim 2.5$ fm) these finite size effects are a likely origin of that discrepancy.

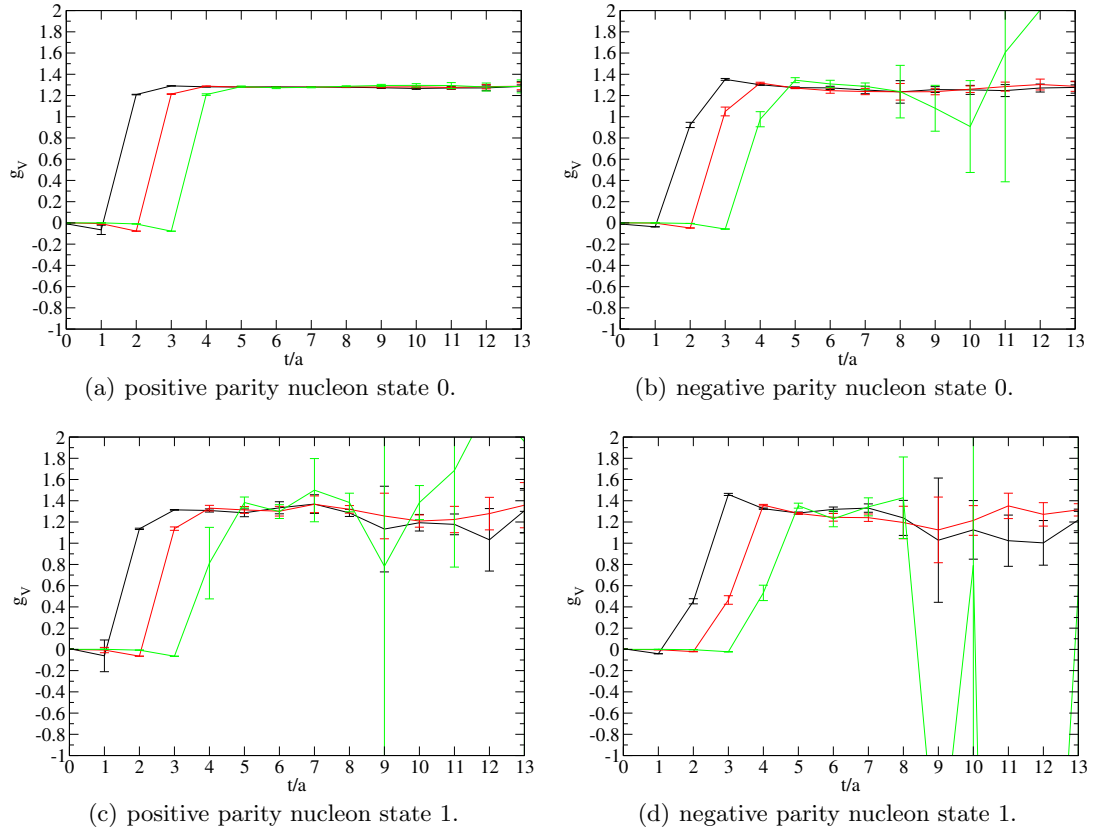
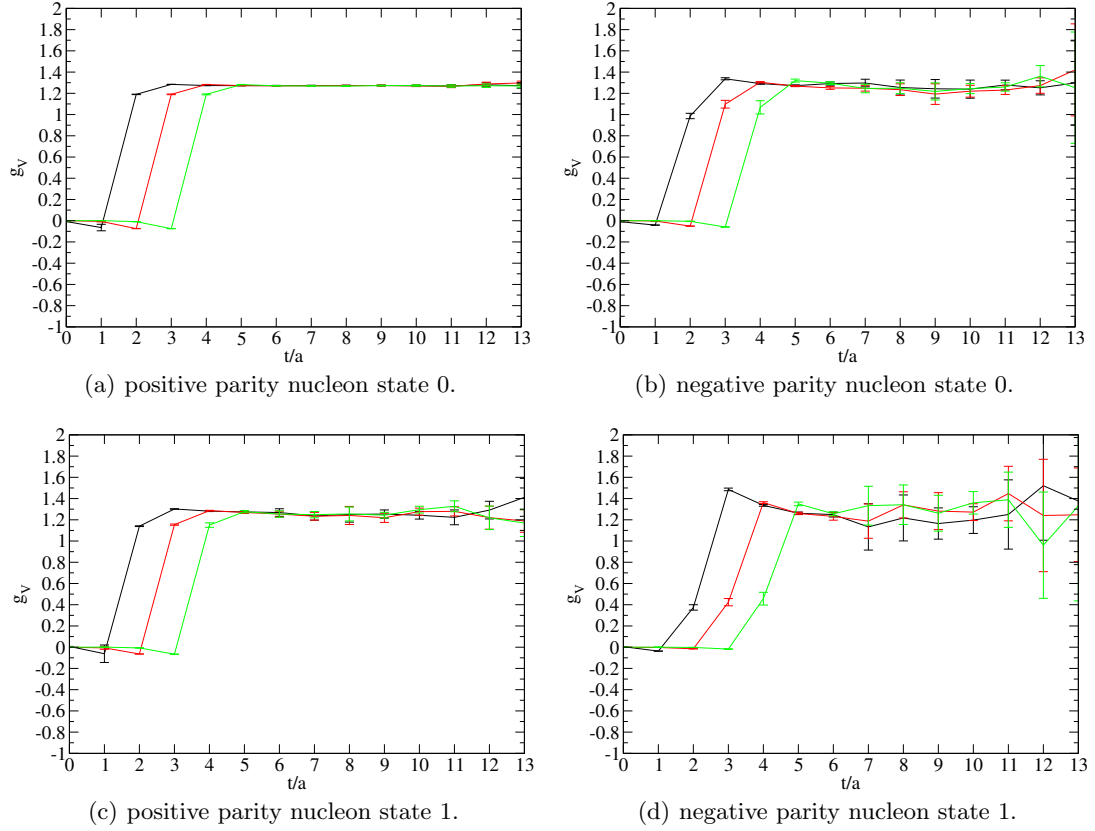
We observe two approximately degenerate negative-parity states in the region of the $N^*(1535)$ and $N^*(1650)$ resonances. The most important point is that we indeed obtain one negative parity state with a very small value of g_A . Such a small value is consistent with approximate chiral restoration, that was initially suggested for the highly excited states [12, 13, 14]. If the negative parity state that we observe is indeed a signal of the approximately restored chiral symmetry, then there must be its chiral partner of positive parity with small axial charge in the same energy region. This could be a possible scenario for the Roper resonance that has so far escaped clear identification on the lattice.

The quark model predicts for the axial charges of the resonances $N^*(1535)$ and $N^*(1650)$ the values $-1/9$ and $5/9$, respectively [52, 53]. Consequently our small axial charge is also consistent with the quark model axial charge of $N^*(1535)$.

The axial charge of the other observed negative parity state is large, close to the nucleon's axial charge. Thus our result is inconsistent with result of [1]. It is also inconsistent with both the chiral restoration scenario in this state, as well as with the quark model prediction. A similarity of the axial charge of this state with the nucleon's axial charge suggests the following interpretation of this state. The axial charge of the πN system in the S -wave state should be close to the nucleon's axial charge since the axial charge of the pion is 0. This hints that this state is in fact not a resonance, but rather a πN system in a relative S -wave motion. Indeed, the energy of such a continuum state at present quark masses is the same as the energies of both our observed negative-parity states [36]. For a firm conclusion on this issue one needs additional dy-

**Fig. 6.** Axial charges for ensemble C77, for explanations see text**Fig. 7.** Axial charge for ensemble C72

**Fig. 8.** Axial charge for ensemble C64**Fig. 9.** Axial charge for ensemble A50

**Fig. 10.** Vector charge for ensemble C72**Fig. 11.** Vector charge for ensemble C64

namical observables for both negative-parity states: e.g., their magnetic moments.

ensemble	parity	state	$g_A^{\text{ren,ext}}$
C	+	0	1.128(18)
C	+	1	0.63(22)
C	-	0	1.05(13)
C	-	1	0.062(16)

Table 6. Axial charges of excited nucleons on ensemble C77.

6 Conclusions & Perspectives

We presented the first calculation for g_A of negative-parity nucleon states using dynamical, approximately chiral (CI) fermions. We found a negative-parity state with small axial charge, as predicted by the chiral symmetry restoration hypothesis [12]. Such a small axial charge is also consistent with the axial charge of the $N^*(1535)$ predicted by the quark model. This observation confirms the lattice results obtained by Takahashi et al. [1] with Wilson fermions, which suggests that the chiral symmetry violation inherent for Wilson fermions has no significant effect for that calculation. From our calculation one cannot identify this state with either the $N^*(1535)$ or the $N^*(1650)$. Our result for the ground state nucleon g_A is rather close to the physical value. We attribute the remaining discrepancy to finite volume effects.

The second observed negative-parity state has practically the same axial charge as the nucleon. This suggests that this state may not be a resonance, but a πN system in the S -wave of relative motion. Further studies of this interesting issue are required for a firm conclusion.

As this was a pioneering study with dynamical CI fermions, it can be improved in many ways by future work. Most obviously, our analysis was based on an very small number of configurations and very few ensembles which strongly limited our possibilities to control the chiral, continuum and infinite-volume extrapolations. Substantially more statistics would clearly help. However, of equal importance is the optimal choice of sources for such studies. The results of our analysis suggest that there is room for improvement. Actually, this is not just a technical issue. From the different overlap with various sources one can try to deduce at least qualitative information about the structure of the wavefunctions of hadron states, information which one can hardly get in any other way. More specifically, our results suggest that the wavefunction of the negative-parity state with very small axial charge is compact because it has large overlap with a very narrow source. This is consistent with our interpretation that the other negative-parity state represents a πN state. To obtain more insight, it would also be interesting to repeat this analysis with other sources, in particular with sources which contain derivatives. Derivative sources have been shown to improve lattice determinations of excited-meson properties; see [54,55].

7 Acknowledgements

This work was supported by the COSY FFE program under contract number 41821484 (COSY-0104). L.Y.G. acknowledges support from the Austrian Science Fund (FWF) through Grant No. P21970-N16.

8 References

References

1. T.T. Takahashi, T. Kunihiro, Nucl. Phys. Proc. Suppl. **186**, 113 (2009), 0911.2543
2. S. Godfrey, S.L. Olsen, Ann.Rev.Nucl.Part.Sci. **58**, 51 (2008), 0801.3867
3. N. Brambilla, S. Eidelman, B. Heltsley, R. Vogt, G. Bodwin et al., Eur.Phys.J. **C71**, 1534 (2011), 1010.5827
4. A. Ali, W. Wang, Phys.Rev.Lett. **106**, 192001 (2011), 1103.4587
5. A. Ali, C. Hambrock, S. Mishima, Phys.Rev.Lett. **106**, 092002 (2011), 1011.4856
6. C. An, D. Riska, Eur.Phys.J. **A37**, 263 (2008), 0804.4773
7. S.G. Yuan, C.S. An, J. He, Commun.Theor.Phys. **54**, 697 (2010), 0908.2333
8. C. an, Q. Li, D. Riska, B. Zou, Phys.Rev. **C74**, 055205 (2006), nucl-th/0610009
9. B. Liu, B. Zou, Phys.Rev.Lett. **96**, 042002 (2006), nucl-th/0503069
10. C. An, B. Zou, Eur.Phys.J. **A39**, 195 (2009), 0802.3996
11. R.L. Jaffe, D. Pirjol, A. Scardicchio, Phys. Rept. **435**, 157 (2006), hep-ph/0602010
12. L.Y. Glozman, Phys. Lett. **B475**, 329 (2000), hep-ph/9908207
13. T.D. Cohen, L.Y. Glozman, Phys. Rev. **D65**, 016006 (2001), hep-ph/0102206
14. L.Y. Glozman, Phys. Rev. Lett. **99**, 191602 (2007), 0706.3288
15. M. Lüscher, U. Wolff, Nucl. Phys. B **339**, 222 (1990)
16. C. Michael, Nucl. Phys. B **259**, 58 (1985)
17. C. Gatttringer, C. Hagen, C.B. Lang, M. Limmer, D. Mohler, Phys.Rev. **D79**, 054501 (2009), 0812.1681
18. T. Burch et al., Phys. Rev. **D74**, 014504 (2006), hep-lat/0604019
19. T. Burch, C. Gatttringer, L.Y. Glozman, C. Hagen, C.B. Lang et al., Phys.Rev. **D73**, 094505 (2006), hep-lat/0601026
20. R.G. Edwards, J.J. Dudek, D.G. Richards, S.J. Wallace (2011), 1104.5152
21. J. Bulava, R. Edwards, E. Engelson, B. Joo, H.W. Lin et al., Phys.Rev. **D82**, 014507 (2010), 1004.5072
22. M. Mahbub, W. Kamleh, D.B. Leinweber, P.J. Moran, A.G. Williams (CSSM Lattice collaboration) (2010), 1011.5724
23. H.W. Lin, S.D. Cohen (2011), * Temporary entry *, 1108.2528
24. S. Beane, E. Chang, W. Detmold, H. Lin, T. Luu et al., Phys.Rev. **D84**, 014507 (2011), 1104.4101
25. C.B. Lang, D. Mohler, S. Prelovsek, M. Vidmar, Phys. Rev. **D84**, 054503 (2011), 1105.5636
26. T.T. Takahashi, T. Kunihiro, Phys. Rev. **D78**, 011503 (2008), 0801.4707

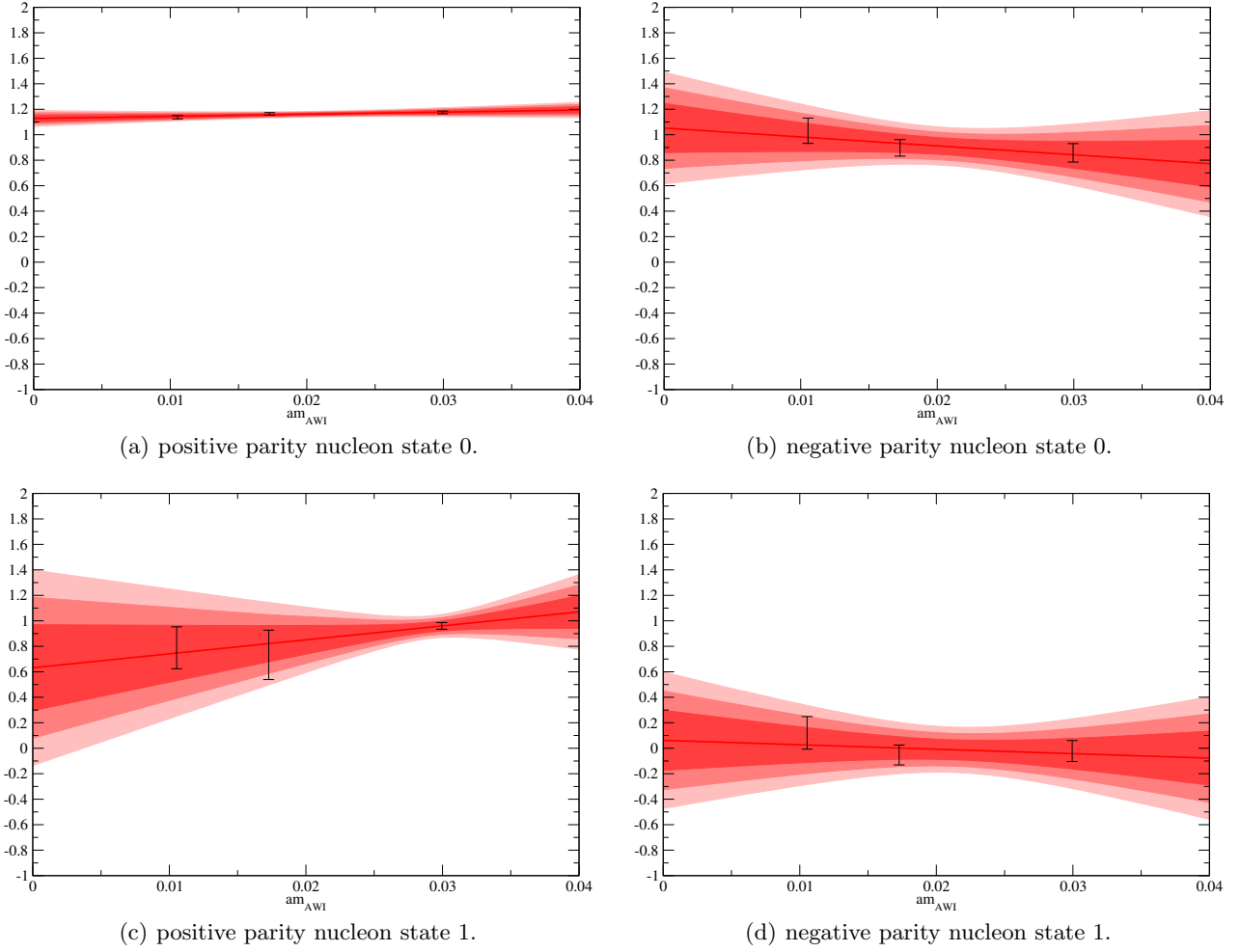


Fig. 12. Extrapolation of the renormalized axial charge for ensemble C. We show data points as well as 1, 2 and 3σ error bands.

27. C. Gatttringer, Phys. Rev. **D63**, 114501 (2001), [hep-lat/0003005](#)
28. C. Gatttringer, I. Hip, C.B. Lang, Nucl. Phys. **B597**, 451 (2001), [hep-lat/0007042](#)
29. F. Bruckmann, N. Cundy, F. Gruber, T. Lippert, A. Schäfer (2011), * Temporary entry *, 1107.0897
30. K. Hagiwara et al. (Particle Data Group), Phys. Rev. **D66**, 010001 (2002)
31. S. Sasaki, K. Orginos, S. Ohta, T. Blum (the RIKEN-BNL-Columbia-KEK), Phys. Rev. **D68**, 054509 (2003), [hep-lat/0306007](#)
32. B. Blossier, G. von Hippel, T. Mendes, R. Sommer, M. Della Morte, PoS **LATTICE2008**, 135 (2008), 0808.1017
33. G.P. Engel, C.B. Lang, M. Limmer, D. Mohler, A. Schäfer (2011), 1112.1601
34. D. Brömmel et al. (Bern-Graz-Regensburg), Nucl. Phys. Proc. Suppl. **129**, 251 (2004), [hep-lat/0309036](#)
35. T. Burch, C. Hagen, C.B. Lang, M. Limmer, A. Schäfer, Phys. Rev. **D79**, 014504 (2009), 0809.1103
36. G.P. Engel, C.B. Lang, M. Limmer, D. Mohler, A. Schäfer, PoS **LATTICE2010**, 103 (2010), 1010.2366
37. R. Sommer, Nucl. Phys. **B411**, 839 (1994), [hep-lat/9310022](#)
38. M. Guagnelli, R. Sommer, H. Wittig (ALPHA), Nucl. Phys. **B535**, 389 (1998), [hep-lat/9806005](#)
39. C. Morningstar, M.J. Peardon, Phys. Rev. **D69**, 054501 (2004), [hep-lat/0311018](#)
40. A. Hasenfratz, F. Knechtli, Phys. Rev. **D64**, 034504 (2001), [hep-lat/0103029](#)
41. C.R. Allton et al. (UKQCD), Phys. Rev. **D47**, 5128 (1993), [hep-lat/9303009](#)
42. C. Best et al., Phys. Rev. **D56**, 2743 (1997), [hep-lat/9703014](#)
43. A. Stathopoulos, K. Orginos, SIAM J.Sci.Comput. **32**, 439 (2010), 0707.0131
44. T. Maurer et al. (2011), to be published
45. T. Yamazaki et al. (RBC+UKQCD Collaboration), Phys.Rev.Lett. **100**, 171602 (2008), 0801.4016
46. P. Hagler, Phys.Rept. **490**, 49 (2010), 0912.5483
47. T. Yamazaki, Y. Aoki, T. Blum, H.W. Lin, S. Ohta et al., Phys.Rev. **D79**, 114505 (2009), 0904.2039
48. H.W. Lin, T. Blum, S. Ohta, S. Sasaki, T. Yamazaki, Phys.Rev. **D78**, 014505 (2008), 0802.0863
49. M. Göckeler et al. (QCDSF/UKQCD Collaboration), PoS **LATTICE2010**, 163 (2010), 1102.3407
50. A. Khan, M. Göckeler, P. Hagler, T. Hemmert, R. Horsley et al., Phys.Rev. **D74**, 094508 (2006), [hep-lat/0603028](#)

- 51. R. Jaffe, Phys.Lett. **B529**, 105 (2002), [hep-ph/0108015](#)
- 52. L.Y. Glozman, A.V. Nefediev, Nucl. Phys. **A807**, 38 (2008), [0801.4343](#)
- 53. K.S. Choi, W. Plessas, R.F. Wagenbrunn, Phys. Rev. **C81**, 028201 (2010), [0908.3959](#)
- 54. C. Gatttringer, L.Y. Glozman, C.B. Lang, D. Mohler, S. Prelovsek, Phys. Rev. **D78**, 034501 (2008), [0802.2020](#)
- 55. C. Gatttringer, L.Y. Glozman, C.B. Lang, D. Mohler, S. Prelovsek, PoS **LAT2007**, 123 (2007), [0709.4456](#)